Plant, Cell and Environment (2006) **29**, 535–545 doi: 10.1111/j.1365-3040.2005.01430.x

Adjustments in hydraulic architecture of *Pinus palustris* maintain similar stomatal conductance in xeric and mesic habitats

R. N. ADDINGTON[1,2], L. A. DONOVAN[1], R. J. MITCHELL[2], J. M. VOSE[3], S. D. PECOT[2], S. B. JACK[2], U. G. HACKE[4], J. S. SPERRY[4] & R. OREN[5]

[1]Department of Plant Biology, University of Georgia, Athens, GA 30602, USA, [2]Joseph W. Jones Ecological Research Center, Newton, GA 39870, USA, [3]USDA Forest Service, South-eastern Forest Experiment Station, Coweeta Hydrologic Laboratory, Otto, NC 28763, USA, [4]Department of Biology, University of Utah, Salt Lake City, UT 84112, USA and [5]Nicholas School of the Environment and Earth Sciences, Duke University, Durham, NC 27708, USA

ABSTRACT

We investigated relationships between whole-tree hydraulic architecture and stomatal conductance in *Pinus palustris* Mill. (longleaf pine) across habitats that differed in soil properties and habitat structure. Trees occupying a xeric habitat (characterized by sandy, well-drained soils, higher nitrogen availability and lower overstory tree density) were shorter in stature and had lower sapwood-to-leaf area ratio (A_S:A_L) than trees in a mesic habitat. The soil-leaf water potential gradient ($\Psi_S - \Psi_L$) and leaf-specific hydraulic conductance (k_L) were similar between sites, as was tissue-specific hydraulic conductivity (K_S) of roots. Leaf and canopy stomatal conductance (g_S and G_S, respectively) were also similar between sites, and they tended to be somewhat higher at the xeric site during morning hours when vapour pressure deficit (D) was low. A hydraulic model incorporating tree height, A_S:A_L and $\Psi_S - \Psi_L$ accurately described the observed variation in individual tree G_{Sref} (G_S at $D = 1$ kPa) across sites and indicated that tree height was an important determinant of G_{Sref} across sites. This, combined with a 42% higher root-to-leaf area ratio (A_R:A_L) at the xeric site, suggests that xeric site trees are hydraulically well equipped to realize equal – and sometimes higher – potential for conductance compared with trees on mesic sites. However, a slightly more sensitive stomatal closure response to increasing D observed in xeric site trees suggests that this potential for higher conductance may only be reached when D is low and when the capacity of the hydraulic system to supply water to foliage is not greatly challenged.

Key-words: habitat structure; hydraulic conductance; leaf water potential; longleaf pine; stand density; tree height; water relations.

Correspondence: Robert Addington. Present address: The Nature Conservancy, P.O.Box 52452, Fort Benning, GA31995, Phone: +1 706 5447515 Fax: +1 706 5446570; e-mail: raddington@tnc.org

INTRODUCTION

Stomatal conductance is well-correlated with hydraulic conductance along the soil to leaf pathway (Sperry, Alder & Eastlack 1993; Saliendra, Sperry & Comstock 1995; Bond & Kavanagh 1999; Meinzer *et al*. 1999; Hubbard *et al*. 2001). Hydraulic conductance (leaf-specific; k_L), in turn, is closely linked to plant hydraulic architecture, including sapwood-to-leaf area ratio (A_S:A_L), root-to-leaf area ratio (A_R:A_L), tissue-specific hydraulic conductivity (K_S) and plant stature or height (h) (Andrade *et al*. 1998; Ewers, Oren & Sperry 2000; Hacke *et al*. 2000; Schäfer, Oren & Tenhunen 2000; Maherali & DeLucia 2001; Mencuccini 2003). Increases in k_L are correlated with increases in A_S:A_L, A_R:A_L and K_S. Furthermore, k_L has been shown to decrease with increasing tree height. Such adjustments in hydraulic architecture are influenced by environment and occur to balance k_L and leaf gas exchange with avoidance of xylem dysfunction and hydraulic failure (Sperry *et al*. 2002; Katul, Leuning & Oren 2003).

A host of environmental variables have been shown to influence hydraulic architecture. Soil water limitation, for example, promotes biomass allocation below ground, thereby increasing standing root crop and A_R:A_L (Comeau & Kimmins 1989; Gower *et al*. 1994; Albaugh *et al*. 1998; Hacke *et al*. 2000). Plants occupying more arid habitats maintain higher A_S:A_L than plants growing in areas where atmospheric moisture is not as limiting (Callaway, DeLucia & Schlesinger 1994; Mencuccini & Grace 1995). Nitrogen fertilization has been shown to encourage leaf area production (Albaugh *et al*. 1998), thereby decreasing both A_R:A_L and A_S:A_L. Soil moisture, aridity and nitrogen availability have all been shown to influence K_S and vulnerability to xylem cavitation in various ways (Alder, Sperry & Pockman 1996; Ewers *et al*. 2000; Hacke *et al*. 2000; Maherali & DeLucia 2000). In addition to resource-related influences, hydraulic architecture has also been shown to vary according to habitat structural influences such as stand density (Whitehead, Jarvis & Waring 1984). Individual tree leaf area (A_L), canopy structure, tree height–diameter relation-

ships and biomass allocation among roots, shoots and leaves have all been shown to be influenced by stand density (Pearson, Fahey & Knight 1984; Dean & Long 1986, 1992; Oren *et al*. 1987). These findings in total indicate that adjustments in tree form and hydraulic architecture are made at a variety of scales, from tissues to whole trees to stands. Furthermore, these studies illustrate that the factors influencing hydraulic architecture are complex, and understanding them and their effects on stomatal conductance requires consideration of several habitat components, including resource availability and feedbacks between resource availability and habitat structure. Few studies, however, have evaluated hydraulic architecture and its consequence on stomatal conductance in this entire context.

We investigated factors influencing hydraulic architecture, hydraulic conductance and stomatal conductance for *Pinus palustris* (Mill.) at extreme ends of a resource availability and community composition gradient within the coastal plain region of the south-eastern United States. *P. palustris* has a wide ecological distribution within this region, occupying coarse-textured soils that can be extremely droughty during summer, as well as finer-textured soils often underlain by clay pans. Changes in stand structure are concomitant with changes in soil texture along this gradient. In more mesic habitats, *P. palustris* is the dominant overstory species, forming almost monotypic stands where fire is maintained. Some hardwood species, *Quercus virginiana* (Mill.), for example, are also typical in the midstory (Abrahamson & Hartnett 1990), but their density is generally low depending on the frequency and intensity of fire. In more xeric habitats, *P. palustris* still dominates the overstory, but the density of drought-adapted *Quercus* ssp., primarily *Q. laevis* (Walt.), *Q. margaretta* (Ashe) and *Q. geminata* (Small), increases dramatically in the midstory (Jacqmain, Jones & Mitchell 1999). Overstory density and leaf area indices in these xeric habitats are still much lower relative to mesic habitats (Mitchell *et al*. 1999) and trees in xeric habitats are also shorter in stature. Per cent soil moisture in the upper soil profile is consistently lower at the xeric end of the gradient, yet soil nitrogen mineralization is higher due to higher soil temperature (Wilson *et al*. 1999, 2002).

For *P. palustris* occupying xeric and mesic habitats, we measured the following architectural and physiological variables: A_S:A_L, A_R:A_L, tree height, leaf water potential (Ψ_L), k_L, root K_S, leaf stomatal conductance (g_S) and sap-flux-scaled canopy stomatal conductance (G_S). Stomatal conductance across sites was evaluated in the context of hydraulic architecture using the hydraulic model of Schäfer *et al*. (2000). The goal of the study was to characterize hydraulic and stomatal behaviour under favourable soil moisture conditions in both habitats. We also provide some discussion and speculation about the potential role of drought and soil moisture decline across habitats. We predicted that xeric site trees would exhibit shifts in hydraulic architecture aimed at improving leaf water status, but that stomatal conductance would still be lower in trees occupying xeric versus mesic habitats.

MATERIALS AND METHODS

Study sites

Sites for this study were established in representative xeric and mesic *P. palustris* habitats at the Joseph W. Jones Ecological Research Center in south-west GA, USA (31°N, 84°W). Regional mean daily temperatures range from 21 to 34 °C in summer to 5–17 °C in winter, and mean annual precipitation is 1310 mm (Goebel *et al*. 2001). The two sites are located ≈5 km from one another and they experience similar climate. The sites were defined as xeric and mesic based on the drainage characteristics of their soils and on the composition of the woody plant community. The xeric site occurred on an upland sand ridge and had deep, sandy soils classified as Typic Quartzipsamments, with relatively low water holding capacity (WHC) (18 cm water per m soil in the upper 3 m) and no argillic horizon (i.e. no significant accumulation of clay) within 3 m (Goebel *et al*. 2001). This site measured 1.32 ha and contained 71 pine trees and 494 oak trees, the majority of which were *Q. laevis*. The mesic site occurred on an upland terrace and had soils classified as Aquic Arenic Kandiudults, with higher WHC (40 cm water per m soil in the upper 3 m) and an argillic horizon within 0.5 m of the soil surface (Goebel *et al*. 2001). These soils were sandy loam over sandy clay loam or clay. The site established in this habitat contained 121 pine trees and no oaks over an area of 0.53 ha. Soil texture fractions (per cent sand, silt, clay) for both sites for the upper 1 m soil are reported in Goebel *et al*. (2001) and are shown in Table 1. Saturated soil hydraulic conductivity (K_{Soil}) was measured at three depth intervals (0–40, 41–100 and 101–200 cm) at three locations per site using a compact constant head permeameter (Amoozemeter, Ksat, Inc., Raleigh, NC, USA). Stand inventory measurements, including stand density, basal area, mean tree diameter at breast height (DBH), mean tree height and mean age were made for both sites prior to the study (Mitchell *et al*. 1999) and are also presented in Table 1. Stands at both sites are multi-aged. Scaffold towers were constructed prior to the study, permitting canopy access to three *P. palustris* trees on each site. Both sites were managed using prescribed fire and were burned in winter 2000 prior to sampling.

A_L

Tree A_L (m^2) was estimated for each site using site-specific allometric equations developed at the beginning of the 2000 growing season. Branch harvests were conducted during January–February 2000 on 15 and 17 xeric and mesic site trees, respectively. Trees representing the full range of sizes present on each site were randomly selected along transects adjacent to each site. The diameter of every branch in each tree was measured by climbing the trees, and six branches per tree (two per crown third) were randomly selected and cut. Needles from cut branches were collected and dried in the laboratory to constant mass (g) at 70 °C. Projected A_L (cm^2) was measured on a subsample of fresh needles from each branch using a leaf area meter (LI-3100, Li-Cor

Table 1. Soil and stand characteristics for xeric and mesic habitats. Soil texture fraction (per cent sand, silt, clay) and WHC represent means ($n = 3$ measurement locations per site; ±1 SE) taken from Goebel *et al*. (2001).

		Xeric	Mesic
Soil characteristics			
Sand fraction (%)		89.3 (0.8)	63.4 (1.5)
Silt fraction (%)		7.1 (1.1)	24.3 (3.1)
Clay fraction (%)		3.7 (0.3)	12.4 (4.6)
WHC (cm m^{-1})		18.0	40.0
K_{Soil} (cm h^{-1})	0–40 cm	49.8 (8.8)	5.3 (0.9)
	41–100 cm	48.7 (13.7)	3.2 (1.2)
	101–200 cm	43.1 (2.2)	0.2 (0.04)
Stand (characteristics for *Pinus palustris*)			
Density (trees ha^{-1})		54	230
Basal area (m^2 ha^{-1})		2.7	10.7
Mean DBH (cm)		24.7 (8.6–49.1)	21.8 (7.5–52.9)
Mean age (years)		57 (7–198)	44 (19–166)
Mean height (m)		13.7 (6.9–20.8)	17.7 (8.3–24.2)
SAI (cm^2 m^{-2})		2.18	7.93
RAI (m^2 m^{-2})		0.67	1.31
LAI (m^2 m^{-2}) (min–max)		0.22–0.39	0.65–1.11
A_S:A_L (cm^2 m^{-2})		5.6	7.1
A_R:A_L (m^2 m^{-2})		1.7	1.2

Saturated soil hydraulic conductivity (K_{Soil}) was measured at three soil depth intervals at $n = 3$ measurement locations per site. Stand characteristics are for *P. palustris* only on each site (*Quercus* spp. codominate xeric site). Values in parentheses for soil characteristics are ± 1 SE. Values in parentheses for the stand characteristics are ranges. Calculation of A_S:A_L and A_R:A_L used estimates of A_L averaged for November–December 2000, corresponding to the period when roots were collected.
WHC, water holding capacity; DBH, diameter at breast height; SAI, sapwood area index; LAI, leaf area index; RAI, root area index for roots < 5 mm in diameter; A_S:A_L, sapwood area to leaf area ratio; A_R:A_L, root area to leaf area ratio.

Instruments, Lincoln, NE, USA). Specific A_L (cm^2 g^{-1}) was then calculated and used to convert bulk needle dry weight to leaf area for each harvested branch. Log–log relationships between branch diameter and branch leaf area were developed from harvested branches at each site and used to predict entire tree A_L via branch summation. Log–log relationships between DBH and A_L were then developed for each site. Site differences in the relationship between DBH and A_L were tested using analysis of covariance (ANCOVA) to determine if the models could be reduced across sites. The slope of the DBH–A_L relationship was significantly different between sites ($P < 0.001$), indicating that separate models were appropriate. These models are shown in Table 2 and were used to estimate A_L of all other trees on each site. Leaf area index (LAI, m^2 projected leaf surface m^{-2} ground) was determined as the sum of A_L for each site divided by ground area. Regular measurements of needle elongation and senescence in the tower-accessible trees on each site by Sheffield *et al*. (2003) were used to estimate seasonal changes in A_L and LAI as described in Addington *et al*. (2004).

Sapwood area (A_S)

A_S (cm^2) was estimated for each site from increment cores collected from 16 trees on the xeric site and 18 on the mesic site during October 2000. Sapwood length was determined by visual inspection of the core and converted to area based on the area of a circle, subtracting the area represented by the heartwood and bark. Log–log relationships between DBH and A_S were developed for each site separately and tested as above to determine if the models could be reduced across sites. In this case, there was no significant difference between the sites regarding the relationship of DBH to A_S ($P = 0.534$), indicating that a single model was appropriate as follows:

$$\log A_S = 1.929 \cdot \log\mathrm{DBH} - 0.1281 \quad (r^2 = 0.97, P < 0.001). \qquad (1)$$

Table 2. Leaf area (A_L, m^2) predictions from DBH (cm) for xeric and mesic site trees determined from pre-growing season branch harvests

Site	*Y*	*X*	*a*	*b*	r^2	*P* (<)	*n*
Xeric	$\log A_L$	logDBH	–0.908	1.854	0.99	0.001	15
Mesic	$\log A_L$	logDBH	–1.192	1.944	0.98	0.001	17

Equations are in the form: $Y = a + b \cdot X$.
DBH, diameter at breast height.

At both sites, A_S for all *P. palustris* trees was estimated and summed to sapwood area index (SAI, cm^2 sapwood area m^{-2} ground) (Table 1). The A_S:A_L presented in Table 1 was calculated by dividing SAI by LAI, using LAI averaged for November–December corresponding to the period when roots were collected.

Root area and K_S

Root area index (RAI, m^2 root surface area m^{-2} ground) and rooting depth distribution were determined in November–December 2000, by excavating 2-m-deep, 2×0.5 m^2 pits adjacent to each site ($n = 5$ pits per site). Roots were collected at 20 cm depth intervals, separated from non-pine species and sorted into four diameter classes: < 1, 1–2, 2–5 and 5–12 mm. The diameter and length of every root > 2 mm (i.e. 2–5- and 5–12-mm-diameter classes) were measured and the area was calculated based on the area of cylinder. For finer roots (< 1- and 1–2-mm-diameter classes), total root length was estimated using ratios of root length per unit dry mass (specific root length, cm g^{-1}) determined for subsamples in each depth class on each site. Area was then calculated based on the area of a cylinder using the mid-point of each diameter class. Scaling from the pit to the stand level was then achieved as follows: a geographic information system (GIS) calculated the total number of 2×0.5 m^2 polygons that could be drawn within each stand and then measured the distance from the centre of each polygon to the nearest *P. palustris* tree. 'Distance to nearest tree' classes were then derived based on a frequency distribution, and pit locations were chosen to represent each of these classes. To estimate RAI, total root area from each pit was weighted by the proportion of total polygons represented by each class (i.e. number of polygons in each class relative to the total number of polygons). Only roots < 5 mm were used to estimate RAI (Ewers *et al*. 2000; Hacke *et al*. 2000). Estimates in Table 1 represent the root area summed over the 2 m depth profile per unit ground area. The A_R:A_L was calculated by dividing RAI by LAI, again using LAI averaged for November–December

K_S (kg m^{-1} s^{-1} MPa^{-1}) was measured on six roots, < 5 mm in outer diameter, per site. These measurements represent root xylem axial conductivity. Roots were collected in the upper 0.2 m soil on each site and K_S was measured for different xylem cavitation-inducing pressures simulated in the laboratory via the centrifugal force method described in Alder *et al*. (1997) and Hacke *et al*. (2000).

Ψ_L and g_S

Ψ_L (MPa) and g_S (mmol m^{-2} s^{-1}) were measured in the upper canopy thirds of the three tower-accessible trees on each site throughout the growing season, March–October 2000. Pre-dawn, midmorning and midday measurements of Ψ_L were made approximately every 2 weeks using a pressure chamber (Model 1002, PMS Instruments, Corvallis, OR, USA). Mid-morning and midday measurements of g_S were made every 4–5 weeks using a portable infrared gas analyser (IRGA) equipped with an artificial light source (Model LI-6400, Li-Cor Instruments). To isolate the influence of hydraulic architecture on g_S, the influence of environmental variables on g_S had to be removed. This was done by holding photon flux density at a constant 1000 μmol m^{-2} s^{-1} inside the chamber, and maintaining CO_2 concentration at 350 μmol. Needle temperature and relative humidity (RH), however, were allowed to vary with atmospheric conditions so that data would be collected over a range of vapour pressure deficit (D). The D range was 0.99–4.67 kPa on the xeric site (median = 2.41 kPa) and 1.18–4.45 kPa on the mesic site (median = 2.65 kPa). A boundary line analysis was done at the end of the season to depict the upper boundary of the response of g_S to D for each tree (Schäfer *et al*. 2000). This analysis removed the influence of all other environmental variables on the response of g_S to D, including effects of a drought that occurred early in the growing season (Addington *et al*. 2004). A reference g_S (g_{Sref}), defined as g_S at 1 kPa D, was then generated by fitting the data to the functional form:

$$g_S = b - m \cdot \ln D, \quad (2)$$

where the y-intercept represents g_S at 1 kPa D, and the slope of the relationship between g_S and $\ln D$ ($-dg_S/d\ln D$), represents the sensitivity of the stomatal response to D (Oren *et al*. 1999). Measurements of g_S were made on both previous- and current-year needles once new needles reached at least 50% of total elongation. This occurred in August 2000. All measurements of g_S are reported on a leaf area basis, determined by measuring needle radius using digital calipers and calculating all-sided leaf area inside the chamber assuming a cylindrical needle shape (Svenson & Davies 1992).

G_S and k_L

G_S (mmol H_2O m^{-2} s^{-1}) was calculated from measurements of sap flux density (J_S, g m^{-2} s^{-1}) made in the xylem of seven trees on each site during September 2000. Trees were selected to represent the range of tree sizes present on each site and included the three tower-accessible trees on each site (Table 3). Xeric site measurements took place on 2–4, 8–14 and 29 September while mesic site measurements were conducted on 3, 9, 12–14 and 26–29 September. Thermal dissipation probes (TDPs) (Model TDP30, Dynamax, Inc., Houston, TX, USA) were used to measure J_S based on the technique of Granier (1987). Probes were installed in the outer 30 mm of hydroactive xylem at a stem height of 1.3 m on the north side of all trees. Variation in J_S with radial depth was evaluated for the three tower trees on each site by installing north-facing TDPs at 30–60 mm sapwood depth. These measurements were made on 28–30 August, prior to the September measurements. To scale J_S across the entire radial profile, the per cent of hydroactive xylem represented by 0–30 and 30–60 mm sapwood depths were plotted against per cent flux measured at these depths (Ford *et al*. 2004a). Per cent flux beyond 60 mm sapwood depth was then determined based on per cent of hydroactive

Table 3. Response of stomatal conductance at leaf (g_S) and canopy (G_S) scales to vapour pressure deficit (D) in xeric and mesic site trees of various DBH, tree heights (ht) and ages.

Site	DBH (cm)	Ht (m)	Age (year)	g_{Sref}	-dg_S/dln$D$	r^2	n	G_{Sref}	-dG_S/dln$D$	r^2	n
Xeric	16.0	11.1	52					86.15	56.19	0.95	17
	20.3	13.6	53					99.48	61.79	0.95	20
	22.3	14.9	55					61.14	43.77	0.91	18
	27.3*	17.0	47	135.10	76.45	0.83	14	31.25	19.38	0.93	16
	30.0*	17.9	44	131.21	69.94	0.78	13	45.96	37.94	0.98	12
	32.6*	20.1	34	130.29	75.45	0.86	16	37.53	26.21	0.95	17
	36.2	17.7	63					74.30	55.92	0.93	17
Mesic	17.5	17.6	46					75.27	65.23	0.97	11
	22.3	18.5	37					66.12	49.42	0.96	14
	26.9	21.0	52					57.68	36.71	0.95	15
	29.4	18.1	57					39.05	33.84	0.97	11
	37.2*	25.7	73	110.27	53.40	0.80	13	30.62	16.09	0.96	07
	39.6*	26.6	70	124.83	69.70	0.77	13	44.64	26.35	0.94	15
	39.8*	24.1	69	119.93	67.17	0.79	14	20.85	12.06	0.97	10

Data were evaluated by fitting the upper boundary of the g_S and G_S response to D to the functional form: $g_S = b - m \cdot \ln D$. This analysis generates a reference stomatal conductance (g_{Sref} and G_{Sref} in mmol m^{-2} s^{-1}) equal to g_S and G_S at 1 kPa D, and a corresponding sensitivity to increasing D equal to the slope of the g_S and G_S response to D (-dg_S/dln$D$ and -dG_S/dln$D$ in mmol m^{-2} s^{-1} kPa^{-1}). Leaf data represent measurements made approximately monthly from March–October 2000, while canopy data on each site is for several days in September 2000. The number of points in each regression relationship is shown in the column labelled n. Trees accessible by canopy scaffold towers are denoted by an asterisk (*).
DBH, diameter at breast height.

xylem beyond 60 mm using a 3-parameter Gaussian function (Ford *et al*. 2004a). Radial profiles for trees on which J_S was measured only in the outer 30 mm xylem were similarly obtained using the Gaussian function to predict radial decline based on per cent of hydroactive xylem measured in each tree. Because radial variation tended to change according to driving force and maximum flux, midday averages were used, corresponding to the time period when J_S was relatively stable and when stored water was less likely to have a large influence on J_S (Oren *et al*. 1998; Ewers & Oren 2000; Ford *et al*. 2004a,b). All probes were insulated from solar radiation using reflective shielding and J_S was recorded every minute and averaged over a 30 min interval using dataloggers (Model CR-10, Campbell Scientific, Inc., Logan, UT, USA). Neither site had a continuous power source, so dataloggers were powered by battery. The measurement dates listed above appear sporadic because days in which batteries were not fully charged were removed from the analysis.

Transpiration per unit leaf area (E_L, kg m^{-2} leaf s^{-1}) was estimated by multiplying whole-tree J_S by A_S:A_L determined for each tree. k_L (kg m^{-2} leaf h^{-1} MPa^{-1}) was calculated for the three tower-accessible trees on each site on two of the measurement days (13–14 September), corresponding to days when Ψ_L was measured. Midday E_L was divided by the midday water potential gradient ($\Psi_S - \Psi_L - h\rho g$), using pre-dawn Ψ_L as a proxy for Ψ_S and correcting for gravitational effects on the water column of height h and density ρ ($h\rho g$). G_S was calculated for all seven trees on each site using the following equation derived from Whitehead & Jarvis (1981):

$$G_S = (G_v T_a \rho E_L)/D, \quad (3)$$

where G_v is the universal gas constant adjusted for water vapour (0.462 m^3 kPa K^{-1} kg^{-1}), T_A is the air temperature in degrees K and ρ is the density of water (998 kg m^{-3}). The Tetens formula (Murray 1967) was used to calculate D from canopy T_A and RH. This calculation substituted T_A for leaf temperature based on the assumption that the canopy and surrounding atmosphere are closely coupled due to the open nature and roughness of the coniferous canopy on both study sites. Both T_A and RH were measured using T_A-RH sensors (Model H8, HOBO Computer Corp., Bourne, MA, USA) affixed to each tower in the upper canopy third. Solar radiation was measured at a weather station located between the sites using a pyranometer (Model LI-200S, Li-Cor Instruments).

Statistical and model analysis

Analysis of covariance (ANCOVA) was employed for testing differences between sites for most variables, including the relationship between DBH and tree height, DBH and A_L, DBH and A_S, soil depth and A_R, D and pre-dawn Ψ_L, D and g_S, and D and G_S. In cases where these relationships were non-linear, variables were log-transformed to meet the assumption of linearity in ANCOVA. Differences among slope coefficients were tested first and if there was no significant difference, tests for differences between intercepts were carried out. All analyses were conducted using individual trees (or pits in the case of root area analyses) within each site and were performed using the general linear model (GLM) procedure in SAS version 8.1 (SAS Institute, Cary, NC, USA). All linear and non-linear curve-fits were made using SigmaPlot software (SigmaPlot v5.0; SPSS, Chicago, IL, USA).

To facilitate comparison of G_S between sites, a boundary line analysis that incorporated solar radiation and D was performed and a reference G_S (G_{Sref}) was determined for each tree, as described for leaf-level g_S measurements. Data where $D < 0.60$ kPa were removed from this analysis to minimize any errors associated with calculating G_S at low D (Ewers & Oren 2000). The range of D over which data was collected and used in this analysis was 0.60–2.51 kPa on the xeric site (median = 1.26 kPa) and 0.60–2.30 kPa on the mesic site (median = 1.07 kPa). The influence of hydraulic architecture on stomatal conductance across sites was then evaluated using G_{Sref} and the hydraulic model of Schäfer *et al*. (2000):

$$G_{sref} \propto E_L \propto (1/h) \cdot (A_S{:}A_L) \cdot (\Psi_S - \Psi_L - h\rho g). \quad (4)$$

The model assumes that k_L is proportional to the term $(1/h) \cdot (A_S{:}A_L)$, that is, k_L is inversely proportional to h or the path length over which water must travel and is directly proportional to A_S or the conducting area. The proportionality to A_S implicitly assumes that the sapwood-area-specific conductivity of the plant trunk does not vary between sites or with age. The bases for these assumptions are described more comprehensively by Schäfer *et al*. (2000). Although we measured K_S in roots and found similarity between sites (see below), these estimates were not included in the model because they represent only the root portion of soil-leaf conductivity. For modelling purposes, $A_S{:}A_L$ was estimated from h using the relationship between $A_S{:}A_L$ and h presented in Fig. 2. The pooled average $\Psi_S - \Psi_L$ across sites was used for the term $\Psi_S - \Psi_L - h\rho g$, and this term was allowed to vary with changes in $h\rho g$. The model predicted a relative change in G_{Sref} expected across trees based on relative changes in each of the input variables. Each input variable was normalized by its average across trees to derive this relative change. The relative variation in G_{Sref} predicted by the model for each tree was then multiplied by the average actual G_{Sref} across trees to generate the dashed line in Fig. 8.

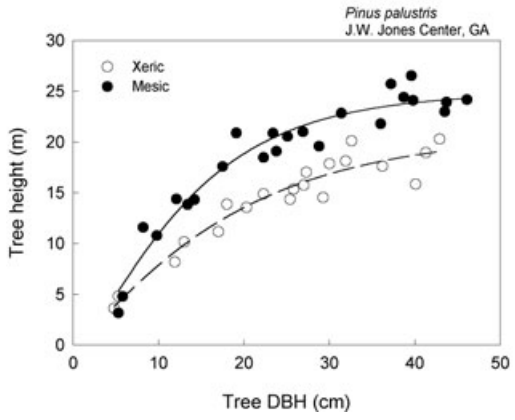

Figure 1. Tree height versus tree diameter at breast height (DBH) for trees on xeric and mesic sites.

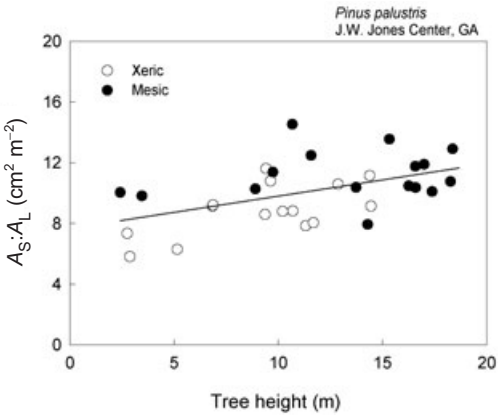

Figure 2. Increase in sapwood to leaf area ratio ($A_S{:}A_L$) with increasing tree height for trees occupying xeric and mesic sites.

RESULTS

Maximum pine LAI occurred in September for both sites and was nearly a third at the xeric relative to the mesic site, reflecting the lower density of pine at the xeric site (Table 1). Leaf area per tree at a given DBH was significantly higher at the xeric site ($P < 0.001$), but sapwood area per DBH was similar ($P = 0.534$), leading to lower $A_S{:}A_L$ for xeric site trees compared to those on the mesic site (Table 1). Tree height for a given DBH was significantly lower on the xeric site ($P < 0.001$; Fig. 1), and the increase in $A_S{:}A_L$ from the xeric to the mesic site was positively, though weakly, correlated with the increase in tree height across stands ($r^2 = 0.26$, $P < 0.01$; Fig. 2). The relationship between $A_S{:}A_L$ and tree height was more obvious within the xeric stand than within the mesic stand (Fig. 2).

Pine RAI was lower on the xeric site, again reflecting the lower pine density on this site, but this is likewise compensated for by a higher amount of mean root area per individual tree (Table 1). The analysis revealed no site by soil depth interaction ($P = 0.187$), indicating that the stands had similar root distribution with depth (Fig. 3). Although both total root and leaf areas were lower at the xeric site, $A_R{:}A_L$ was 42% higher on this site relative to the mesic site (Table 1). There was no significant difference between sites in the response of K_S of roots to xylem pressure ($P = 0.771$), and no significant difference in maximum K_S at a given xylem pressure ($P = 0.324$), though mean maximum K_S was slightly higher on the xeric site (Fig. 4).

Ψ_L varied with D, but no site differences were observed in the relationship between Ψ_L and D ($P = 0.441$). Ψ_L at a given D was similar at both sites ($P = 0.231$), though Ψ_L tended to be slightly less negative on the xeric site, particularly before dawn when D was low (Fig. 5). Mean predawn Ψ_L over the course of the measurement period was –0.49 and –0.58 MPa for the xeric and mesic sites, respectively. Mean mid-morning Ψ_L was –1.06 and –1.12 MPa, and mean midday Ψ_L was –1.58 and –1.67 MPa for xeric and mesic, respectively. The soil-leaf water potential gradient ($\Psi_S - \Psi_L$) was likewise similar between the sites (1.08 and

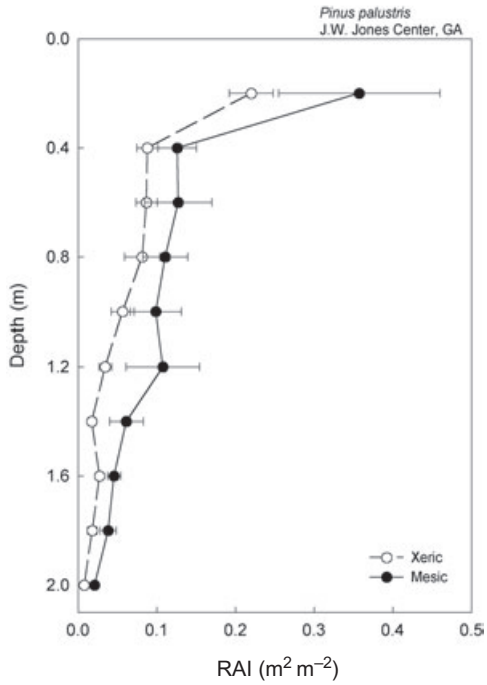

Figure 3. Root area index (RAI) of *Pinus palustris* roots < 5 mm diameter at 0.2 m depth intervals for xeric and mesic sites. Values represent the mean of $n = 5$ excavation pits per site (± 1 SE).

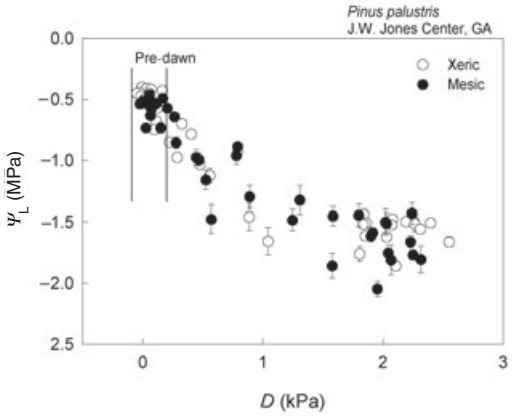

Figure 5. Leaf water potential (Ψ_L) at a given vapour pressure deficit (D) for xeric and mesic sites measured biweekly, March–October 2000. Values represent mean of $n = 3$ trees per site (± 1 SE).

1.09 MPa for xeric and mesic, respectively). Incorporating the effect of gravity on the $\Psi_S - \Psi_L - h\rho g$ (using 0.01 MPa per m tree height), however, showed that xeric site trees had a slightly higher average driving force for water flow owing to their shorter stature (0.90 and 0.84 MPa for xeric and mesic, respectively). k_L was similar between the sites (t-test, $P = 0.232$; Fig. 6)

The response of g_S to D was also similar between sites (slopes comparison, $P = 0.239$), and there was no significant difference in g_S at a given D (intercepts comparison, $P = 0158$; Fig. 7). Again, however, g_S tended to be higher at low D on the xeric site and showed a somewhat more sensitive stomatal response to increasing D. At the reference D ($D = 1$ kPa), g_S averaged 13% higher on the xeric site compared to the mesic site (132.20 versus 117.67), and the average slope of the g_S to ln$D$ response ($-dg_S/d\ln D$) was 73.97 and 63.42 for the xeric and mesic sites, respectively (Table 3). There was no significant difference between needle-age classes (current- versus previous-year needles) in the response of g_S to D for either site (minimum $P = 0.106$).

Patterns in g_S and response to D observed between sites at the leaf level were similar at the canopy level. G_S at the xeric site showed a slightly more sensitive stomatal response to increasing D, though there was no significant difference in the overall response of G_S to D between sites ($P = 0.651$). The average slope of the G_S response to ln$D$ ($-dG_S/d\ln D$) was 43.03 and 34.24 for the xeric and mesic sites, respectively (Table 3). At 1 kPa D, G_S (= G_{Sref}) was an average 30% higher on the xeric site compared to the mesic site (62.26 versus 47.75), yet there was no statistically sig-

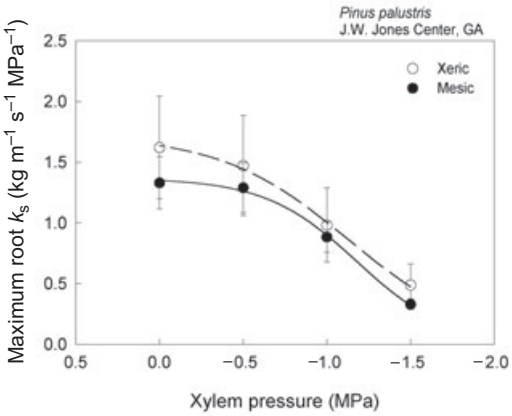

Figure 4. Response of tissue specific hydraulic conductivity (K_S) of roots < 5 mm diameter to increasingly negative root xylem pressure for $n = 6$ (means ± 1 SE) xeric and mesic site roots.

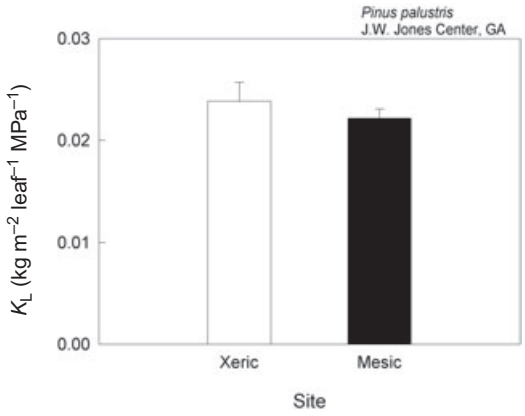

Figure 6. Leaf specific hydraulic conductance (k_L) for xeric and mesic sites. Values represent $n = 3$ trees per site (means ± 1 SE) averaged for 13–14 September 2000.

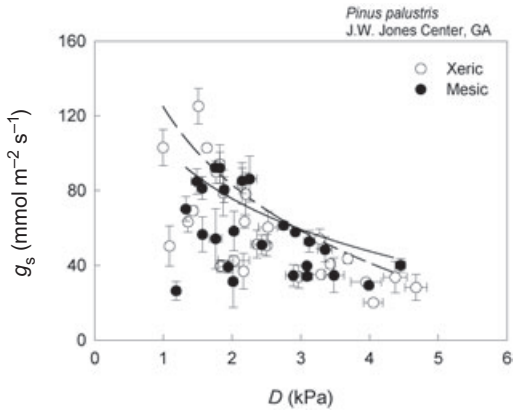

Figure 7. Response of g_S to increasing vapour pressure deficit (D) for previous-year needles on xeric and mesic sites measured monthly, March–October 2000. Values represent mean of $n = 3$ trees per site (± 1 SE), and regression curves represent the upper boundary of the response on both sites.

nificant difference in G_{Sref} between sites ($P = 0.499$). The higher mean G_{Sref} observed on the xeric site appeared largely attributable to differences in tree height. A decline in G_{Sref} with increasing tree height was observed across sites ($r^2 = 0.52$, $P = 0.018$; Fig. 8), implying that a single G_{sref}–tree-height relationship explains the data well across the sites. The predicted decline in G_{Sref} with increasing tree height based on the hydraulic model in Eqn 4 is shown as the dashed line in Fig. 8. Model output closely follows the least square fit to the actual data.

DISCUSSION

To successfully extract and use water, plants that exist across a range of habitats must make adjustments in hydraulic architecture that maintain hydraulic compatibility between plant and environment (Sperry *et al*. 1998; Hacke *et al*. 2000; Maherali & DeLucia 2001; Sperry *et al*. 2002). In the south-eastern United States, *P. palustris* is a species that can be found across a range of habitats, from xeric pine-oak sandhills to more mesic pine-dominated loamhills. We predicted that hydraulically favourable adjustments in architecture would be evident in xeric site trees, but hypothesized that stomatal conductance would be lower in trees occupying xeric versus mesic sites even under favourable soil moisture conditions at both sites. Instead we found that trees at the xeric site supported a mean stomatal conductance equal to and in some cases higher than that measured on the mesic site at both leaf and canopy scales. Thus, the physiological data presented here failed to show the xeric site as obviously more xeric; rather, trees occupying the xeric site exhibited shifts in hydraulic architecture that enabled them to function physiologically similar to their mesic site counterparts.

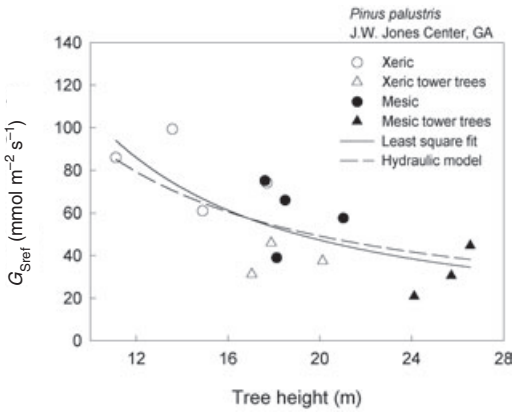

Figure 8. Decline in canopy stomatal conductance at a reference vapour pressure deficit (G_{Sref}, $D = 1$ kPa) with increasing tree height across xeric and mesic sites measured for several days in September 2000. Solid line represents least square fit to the data ($r^2 = 0.52$, $P = 0.0177$), while dashed line shows the expected decline across sites based on observed hydraulic architectural adjustments and the hydraulic model (Eqn 4).

Differences in hydraulic architecture between the sites likely originate as a result of habitat differences in soil properties and habitat structure (Aber, Pastor & Mellilo 1982). Relationships between stand density and individual tree leaf area, canopy structure and tree form are well documented in the literature. For instance, individual tree leaf area and crown volume tend to increase with decreasing stand density (Pearson *et al*. 1984; Whitehead *et al*. 1984; Oren *et al*. 1987), and the formation and ultimate size of trees is dictated by what is required to satisfy mechanical constraints associated with a given tree leaf area and canopy structure (Dean & Long 1986, 1992). Tree height–diameter relationships also follow mechanical-buckling constraints and bending stress (Dean & Long 1986; Osler, West & Downes 1996). Overstory pine density in this study was much lower on the xeric site compared to the mesic site and trees on the xeric site were shorter in stature. Although there was a significant oak component on the xeric site, these species were confined to the midstory and *P. palustris* occupied the overstory without noticeable competition for light. Trees on the xeric site also had longer and wider crowns compared to trees on the mesic site. For the trees in Table 3, live crown ratio and crown width were an average 28 and 17% greater, respectively, on the xeric site (crown data not shown). Individual tree leaf area at a given stem diameter was also higher on the xeric site compared to the mesic site, likely owing to greater crown volume. The trends we observed are consistent with the studies above, but we note that our data are limited to one stand replicate across habitats and would benefit from inclusion of more stand replicates to better understand interactions between stands and individual trees across site types.

Because A_S was similar at both sites, A_S:A_L was lower for individual trees on the xeric site. This ratio adjusts considerably within a species to ensure adequate supply of water to the leaves; it increases as the gap between soil water availability and atmospheric demand for moisture increases, as in arid habitats (Callaway *et al*. 1994; Mencuccini & Grace 1995; Maherali & DeLucia 2001), and as the resistance to soil-leaf water flow increases, as in tall trees

(Ryan *et al*. 2000; Schäfer *et al*. 2000). In our study, differences in A_S:A_L across sites appeared to be due primarily to differences in the height distribution of trees. Consistent with other studies (Schäfer *et al*. 2000; McDowell *et al*. 2002), we observed an increase in A_S:A_L with increasing tree height across sites (Fig. 2). Our use of the hydraulic model (Eqn 4) showed that tree height and A_S:A_L influenced water transport and stomatal conductance in counteracting ways. To illustrate this, the hydraulic model can be modified to represent a predicted ratio of G_{Sref} between sites (G_X/G_M xeric/mesic) based on ratios of input variables as follows:

$$G_X/G_M \propto (h_M/h_X) \cdot (A_X/A_M) \cdot (\Delta\Psi_X/\Delta\Psi_M), \quad (5)$$

where h_M/h_X is the xeric/mesic inverse height ratio, A_X/A_M is the ratio of A_S:A_L and $\Delta\Psi_X/\Delta\Psi_M$ is the ratio $\Psi_S - \Psi_L$ between sites, adjusted for gravity. Using the values in Table 1, h_M/h_X equals 1.29, meaning that in isolation the reduced path length afforded by shorter trees on the xeric site would translate to 29% higher conductance in xeric site trees versus those in the mesic site. The term A_X/A_M equals 0.79, which would result in a similar proportion of stomatal conductance. Combining these two factors in Eqn 5 shows that the effect on mean stomatal conductance of higher A_S:A_L in the mesic stand nearly exactly compensated for the effect of greater tree height (i.e. predicted G_X/G_M is 1.29*0.79 = 1.02). We interpret these results to mean that the site-to-site difference in soil texture and WHC did not affect A_S:A_L directly, but rather indirectly through its effect on stand structure and tree height.

Site differences in soil properties appeared to have no direct effect on $\Psi_S - \Psi_L$ across sites either. In fact, the differences in $\Psi_S - \Psi_L - h\rho g$ between the sites appeared to be mostly driven by the differences in tree height and associated effects of gravity. Applied at a stand level, there was an estimated *enhancement* of conductance of 3% (i.e. $\Delta\Psi_X/\Delta\Psi_M = 1.03$) at the xeric site. This, together with the combined effect of the differences in height and A_S:A_L, would result in a xeric site conductance predicted to be 1.05 that of mesic site trees. The fact that a single relationship between G_{Sref} and tree height in Fig. 8 explains the data well across sites further suggests that the variation we did observe in G_{Sref} is largely attributable to the differences in tree height distribution across sites.

The ratio A_R:A_L also greatly affects the amount of water that can be extracted from the soil (Sperry *et al*. 1998). When stands reach a stage of development in which their leaf and root areas are at maximum, the ratio A_R:A_L at this quasi steady state is highly dependent on soil texture, increasing with increasing sand fraction. Consistent with its sandy texture, xeric site A_R:A_L was 42% higher than the mesic site (Table 1). While this adjustment in A_R:A_L is much less than the five-fold adjustment observed in a similar study in *Pinus taeda* (L) (Hacke *et al*. 2000), it still likely improved water uptake efficiency at the xeric site considerably. It is not possible to assess entirely the effect of higher A_R:A_L on the water economy of *P. palustris* without accounting for water consumption by the oak component also occupying this site. Nevertheless, our results show that at a reference D (= 1 kPa), mean g_{Sref} and G_{Sref} were similar at both sites, or perhaps even higher (13 and 30% for g_{Sref} and G_{Sref}, respectively; Table 3) at the xeric site. The combined above-ground hydraulic adjustments at the xeric site (1.05 that of the mesic site) may not be sufficient to explain the somewhat higher conductance on the xeric site at low D, indicating that below-ground adjustments in hydraulic architecture likely contributed as well. Such below-ground adjustment is consistent with the slightly higher (16%) mean K_S of small roots at the xeric site.

We also assumed that xeric site trees would be deeper rooted than mesic site trees and that proportionately, more root biomass would be found at depth on the xeric site. We found no evidence for this in our 2 m depth pit samples. Yet *P. palustris* is a species known to extend a taproot deep into the soil profile, particularly on sandy sites (Heyward 1933). While we feel our sampling strategy was reasonable for quantifying fine roots within the 2 m depth profile, it was less well suited for determining the depth distribution of the entire rooting profile. Maximum rooting depth is relevant to the current study because of its consequence on hydraulic architecture and water transport; deep rooting may reach additional water resources, but it also increases the path length over which water must be transported. More information is needed to address this issue.

While it appears that *P. palustris* occupying xeric sites are confronted with greater challenges regarding water acquisition relative to trees occupying more mesic sites, adjustments in hydraulic architecture have enabled individual trees on xeric sites to realize equal – and sometimes higher – potential for conductance. The potential for higher conductance at xeric sites may, however, only be reached during times in which D is low and when soil moisture across sites is favourable and does not limit the capacity of the hydraulic system to supply water to foliage. Consistent with this scenario is the observation in this study that as D increased, both g_S and G_S showed a steeper decline in xeric site trees (Table 3). This pattern implies a slightly more sensitive stomatal conductance response to increasing D in xeric site trees, likely necessary to regulate Ψ_L and avoid xylem cavitation (Oren *et al*. 1999). It appears that trees on the xeric site are hydraulically best suited to taking advantage of periods when water is available, but the trade-off is that they may have smaller margins of safety from hydraulic failure during drought and are thus required to show a more sensitive stomatal closure response to increasing soil water limitation (Sperry *et al*. 1998). Future work should parameterize the model of Sperry *et al*. (1998) to evaluate response to declining soil moisture and how changes in hydraulic architecture across sites may influence site water use envelopes and predicted cavitation-inducing transpiration rates (E_{crit}). Differences in root radial resistance across sites should also be considered here. We present results only for root axial resistance, yet root radial resistance can be orders of magnitude greater than axial resistance (Steudle & Peterson 1998). For large woody plants, however, the relative importance of root radial and axial resistance in

limiting transpiration is not well understood due to path length effects. The length over which water must flow radially is much less than the axial length, therefore, the importance of axial resistance should increase with plant size (Sperry *et al*. 2002). Hacke *et al*. (2000) also demonstrate good agreement between whole-plant water use and axial conductivity during water stress, suggesting that differences in root radial resistance across sites and during drought are either negligible or parallel the change in axial resistance.

Lastly, the influence of the oak component on pine hydraulic architecture should be investigated, as these species not only alter stand structure but also nutrient availability. Higher nitrogen availability and mineralization has been reported for the xeric site, believed to be a result of higher quality leaf litter return provided by the oaks, oak root turnover, and higher soil temperatures for mineralization (Wilson *et al*. 2002). By altering nutrient availability relative to the mesic site, oaks on the xeric site may provide a fertilizing effect, encouraging leaf area production in the pines and therefore decreasing A_S:A_L. In this situation, xeric site *P. palustris* may in fact be more sensitive to drought, consistent with the findings of Ewers *et al*. (2000) in *P. taeda* that nitrogen-fertilized stands had smaller margins of safety from predicted hydraulic failure during modelled drought compared to non-fertilized stands. The frequency of drought therefore may be greater for the xeric site relative to the mesic site in this study, meaning that trees on the xeric site may spend proportionately more time in a state of drought relative to mesic site trees. A limited data set collected on these sites during a drought that occurred earlier in the growing season suggests this pattern (Addington 2001), and may explain why longer-term water-use efficiency estimates for these sites indicate that xeric site trees are more water-use efficient compared to mesic site trees (Addington 2001; see also Ford 2004).

The patterns of stomatal behaviour observed in this study suggest that whole-plant architectural and leaf physiological adjustments are well coordinated with one another and with environment and habitat structure. Other studies have demonstrated integration among hydraulic architecture and water transport efficiency to maintain homeostasis (Whitehead *et al*. 1984; Meinzer, Woodruff & Shaw 2004). Our results are consistent with these studies and suggest that interactions among soil properties and stand-level factors such as tree density are important determinants of individual tree form and height, and that hydraulic adjustments across these scales ensure similar site-to-site stomatal capability.

ACKNOWLEDGMENTS

We thank the Robert W. Woodruff Foundation and the Joseph W. Jones Ecological Research Center for supporting this research. We are grateful to Ann Addington, Michael Bell, Aaron DeLong, Barbara Fowler, Virgil Holton, Stacy Hurst, Dan McConville, Ernie Mitchell, Nancy Newberry, Mary Carol Sheffield and Dwan Williams for their help with work in the field and laboratory. We also thank Larry West for loaning equipment, and Karina Schäfer for help in developing the hydraulic model. Chelcy Ford and Tim Harrington provided valuable comments on earlier versions of the manuscript, and comments from Nate McDowell and another anonymous reviewer also considerably improved the manuscript.

REFERENCES

Aber J.D., Pastor J. & Mellilo J.M. (1982) Changes in forest canopy structure along a site quality gradient in southern Wisconsin. *American Midland Naturalist* **108,** 256–265.

Abrahamson W.G. & Hartnett D.C. (1990) Pine flatwoods and dry prairies. In *Ecosystems of Florida* (eds R.L. Myers & J.J. Ewel), pp. 103–149. University of Central Florida Press, Orlando, FL, USA.

Addington R.N. (2001) *Water use patterns and stomatal responses to environment in longleaf pine on contrasting sites*. MS thesis, University of Georgia, Athens, GA, USA.

Addington R.N., Mitchell R.J., Oren R. & Donovan L.A. (2004) Stomatal sensitivity to vapor pressure deficit and its relationship to hydraulic conductance in *Pinus palustris*. *Tree Physiology* **24,** 561–569.

Albaugh T.J., Allen H.L., Dougherty P.M., Kress L.W. & King J.S. (1998) Leaf area and above- and belowground growth responses of loblolly pine to nutrient and water additions. *Forest Science* **44,** 317–328.

Alder N.N., Sperry J.S. & Pockman W.T. (1996) Root and stem xylem embolism, stomatal conductance, and leaf turgor in *Acer gradidentatum* populations along a soil moisture gradient. *Oecologia* **105,** 293–301.

Alder N.N., Pockman W.T., Sperry J.S. & Nuismer S. (1997) Use of centrifugal force in the study of xylem cavitation. *Journal of Experimental Botany* **48,** 665–674.

Andrade J.L., Meinzer F.C., Goldstein G., Holbrook N.M., Cavelier J., Jackson P. & Silvera K. (1998) Regulation of water flux through trunks, branches, and leaves in trees of a lowland tropical forest. *Oecologia* **115,** 463–471.

Bond B.J. & Kavanagh K.L. (1999) Stomatal behavior of four woody species in relation to leaf-specific hydraulic conductance and threshold water potential. *Tree Physiology* **19,** 503–510.

Callaway R.M., DeLucia E.H. & Schlesinger W.H. (1994) Biomass allocation of montane and desert ponderosa pine: an analog for response to climate change. *Ecology* **75,** 1474–1481.

Comeau P.G. & Kimmins J.P. (1989) Above- and below-ground biomass and production of lodgepole pine on sites with differing soil moisture. *Canadian Journal of Forest Research* **19,** 447–454.

Dean T.J. & Long J.N. (1986) Variation in sapwood area-leaf area relations within two stands of lodgepole pine. *Forest Science* **32,** 749–758.

Dean T.J. & Long J.N. (1992) Influence of leaf area and canopy structure on size-density relations in even-aged lodgepole pine stands. *Forest Ecology and Management* **49,** 109–117.

Ewers B.E. & Oren R. (2000) Analysis of assumptions and errors in the calculation of stomatal conductance from sap flux measurements. *Tree Physiology* **20,** 579–589.

Ewers B.E., Oren R. & Sperry J.S. (2000) Influence of nutrient versus water supply on hydraulic architecture and water balance in *Pinus taeda*. *Plant, Cell and Environment* **23,** 1055–1066.

Ford C.R. (2004) *Variable distributions of water as a transpiration source: consequences from the tree stem to ecosystem functioning*. PhD dissertation, University of Georgia, Athens, GA, USA.

Ford C.R., McGuire M.A., Mitchell R.J. & Teskey R.O. (2004a)

Assessing variation in the radial profile of sap flux density in Pinus species and its effect on daily water use. *Tree Physiology* **24,** 241–249.

Ford C.R., Goranson C.E., Mitchell R.J., Will R.E. & Teskey R.O. (2004b) Diurnal and seasonal variability in the radial distribution of sap flow: predicting total stem flow in *Pinus taeda* trees. *Tree Physiology* **24,** 951–960.

Goebel P.C., Palik B.J., Kirkman L.K. & West L. (2001) Forest ecosystems of a lower gulf coastal plain landscape: multifactor classification and analysis. *Journal of the Torrey Botanical Society* **128,** 47–75.

Gower S.T., Gholz H.L., Nakane K. & Baldwin V.C. (1994) Production and carbon allocation patterns of pine forests. *Ecological Bulletins (Copenhagen)* **43,** 115–135.

Granier A. (1987) Evaluation of transpiration in a Douglas-fir stand by means of sap flow measurements. *Tree Physiology* **3,** 309–320.

Hacke U.G., Sperry J.S., Ewers B.E., Ellsworth D.S., Schäfer K.V.R. & Oren R. (2000) Influence of soil porosity on water use in *Pinus taeda*. *Oecologia* **124,** 495–505.

Heyward F. (1933) The root system of longleaf pine on the deep sands of western Florida. *Ecology* **14,** 136–148.

Hubbard R.M., Ryan M.G., Stiller V. & Sperry J.S. (2001) Stomatal conductance and photosynthesis vary linearly with plant hydraulic conductance in ponderosa pine. *Plant, Cell and Environment* **24,** 113–121.

Jacqmain E.I., Jones R.H. & Mitchell R.J. (1999) Influences of frequent cool-season burning across a soil moisture gradient on oak community structure in longleaf pine ecosystems. *American Midland Naturalist* **141,** 85–100.

Katul G., Leuning R. & Oren R. (2003) Relationship between plant hydraulic and biochemical properties derived from a steady-state coupled water and carbon transport model. *Plant, Cell and Environment* **26,** 339–350.

Maherali H. & DeLucia E.H. (2000) Xylem conductivity and vulnerability to cavitation of ponderosa pine growing in contrasting climates. *Tree Physiology* **20,** 859–867.

Maherali H. & DeLucia E.H. (2001) Influence of climate-driven shifts in biomass allocation on water transport and storage in ponderosa pine. *Oecologia* **129,** 481–491.

McDowell N., Barnard H., Bond B.J., *et al.* (2002) The relationship between tree height and leaf area: sapwood area ratio. *Oecologia* **132,** 12–20.

Meinzer F.C., Goldstein G., Franco A.C., Bustamante M., Igler E., Jackson P., Caldas L. & Rundel P.W. (1999) Atmospheric and hydraulic limitations on transpiration in Brazilian Cerrado woody species. *Functional Ecology* **13,** 273–282.

Meinzer F.C., Woodruff D.R. & Shaw D.C. (2004) Integrated responses of hydraulic architecture, water and carbon relations of western hemlock to dwarf mistletoe infection. *Plant, Cell and Environment* **27,** 937–946.

Mencuccini M. (2003) The ecological significance of long-distance water transport: short-term regulation, long-term acclimation and the hydraulic costs of stature across plant life forms. *Plant, Cell and Environment* **26,** 163–182.

Mencuccini M. & Grace J. (1995) Climate influences the leaf area/sapwood area ratio in Scots pine. *Tree Physiology* **15,** 1–10.

Mitchell R.J., Kirkman L.K., Pecot S.D., Wilson C.A., Palik B.J. & Boring L.R. (1999) Patterns and controls of ecosystem function in longleaf pine-wiregrass savannas: I. aboveground net primary productivity. *Canadian Journal of Forest Research* **29,** 743–751.

Murray F.W. (1967) On the computation of saturation vapor pressure. *Journal of Applied Meteorology* **6,** 203–204.

Oren R., Waring R.H., Stafford S.G. & Barrett J.W. (1987) Twenty-four years of Ponderosa pine growth in relation to canopy leaf area and understory competition. *Forest Science* **33,** 538–547.

Oren R., Phillips N., Katul G., Ewers B.E. & Pataki D.E. (1998) Scaling xylem sap flux and soil water balance, and calculating variance: a method for partitioning water flux in forests. *Annales Des Sciences Forestieres* **55,** 191–216.

Oren R., Sperry J.S., Katul G.G., Pataki D.E., Ewers B.E., Phillips N. & Schäfer K.V.R. (1999) Survey and synthesis of intra- and interspecific variation in stomatal sensitivity to vapour pressure deficit. *Plant, Cell and Environment* **22,** 1515–1526.

Osler G.H.R., West P.W. & Downes G.M. (1996) Effects of bending stress on taper and growth of stems of young *Eucalyptus regnans* trees. *Trees* **10,** 239–246.

Pearson J.A., Fahey T.J. & Knight D.H. (1984) Biomass and leaf area in contrasting lodgepole pine forests. *Canadian Journal of Forest Research* **14,** 259–265.

Ryan M.G., Bond B.J., Law B.E., Hubbard R.M., Woodruff D., Cienciala E. & Kucera J. (2000) Transpiration and whole-tree conductance in ponderosa pine trees of different heights. *Oecologia* **124,** 553–560.

Saliendra N.Z., Sperry J.S. & Comstock J.P. (1995) Influence of leaf water status on stomatal response to humidity, hydraulic conductance, and soil drought in *Betula occidentalis*. *Planta* **196,** 357–366.

Schäfer K.V.R., Oren R. & Tenhunen J.D. (2000) The effect of tree height on crown level stomatal conductance. *Plant, Cell and Environment* **23,** 365–375.

Sheffield M.C.P., Gagnon J.L., Jack S.B. & McConville D.J. (2003) Phenological patterns of mature longleaf pine (*Pinus palustris* Miller) under two different soil moisture regimes. *Forest Ecology and Management* **179,** 157–167.

Sperry J.S., Adler F.R., Campbell G.S. & Comstock J.P. (1998) Limitation of plant water use by rhizosphere and xylem conductance: results from a model. *Plant, Cell and Environment* **21,** 347–359.

Sperry J.S., Alder N.N. & Eastlack S.E. (1993) The effect of reduced hydraulic conductance on stomatal conductance and xylem cavitation. *Journal of Experimental Botany* **44,** 1075–1082.

Sperry J.S., Hacke U.G., Oren R. & Comstock J.P. (2002) Water deficits and hydraulic limits to leaf water supply. *Plant, Cell and Environment* **25,** 251–263.

Steudle E. & Peterson C.A. (1998) How does water get through roots? *Journal of Experimental Botany* **49,** 775–788.

Svenson S.E. & Davies F.T., Jr (1992) Comparison of methods for estimating surface area of water-stressed and fully hydrated pine needle segments for gas exchange analysis. *Tree Physiology* **10,** 417–421.

Whitehead D. & Jarvis P.G. (1981) Coniferous forest and plantations. In *Water Deficits and Plant Growth* (ed. T.T. Kozlowski) Vol. VI, pp. 49–152. Academic Press, New York, NY, USA.

Whitehead D., Jarvis P.G. & Waring R.H. (1984) Stomatal conductance, transpiration, and resistance to water uptake in a *Pinus sylvestris* spacing experiment. *Canadian Journal of Forest Research* **14,** 692–700.

Wilson C.A., Mitchell R.J., Boring L.R. & Hendricks J.L. (2002) Soil nitrogen dynamics in a fire-maintained forest ecosystem: results over a 3-year burn interval. *Soil Biology and Biochemistry* **34,** 679–689.

Wilson C.A., Mitchell R.J., Hendricks J.L. & Boring L.R. (1999) Patterns and controls of ecosystem function in longleaf pine-wiregrass savannas. II. nitrogen dynamics. *Canadian Journal of Forest Research* **29,** 752–760.

Received 5 May 2005; received in revised form 22 July 2005; accepted for publication 6 August 2005